

1 ***Modelling and Experimental Investigation of Small-Scale Gasification CHP***  
2 ***Units for Enhancing the Use of Local Biowaste***

3 Oisín de Priall<sup>a\*</sup>, Valentina Gogulancea<sup>a</sup>, Caterina Brandoni<sup>a</sup>, Neil Hewitt<sup>a</sup>, Chris Johnston<sup>b</sup>,  
4 George Onofrei<sup>c</sup>, Ye Huang<sup>a</sup>

5 <sup>a</sup> Centre for Sustainable Technologies, School of the Built Environment, University of Ulster,  
6 Jordanstown, BT37 0QB, UK

7 <sup>b</sup> Agri-Food & Biosciences Institute, Large Park, Hillsborough, Co. Down BT26 6DR,  
8 Northern Ireland, UK.

9 <sup>c</sup> School of Business, Galway-Mayo Institute of Technology, Galway, Ireland

10 \*Corresponding Author at: Centre for Sustainable Technologies, School of the Built  
11 Environment, University of Ulster, Jordanstown, BT37 0QB, UK

12 Email Address: [De\\_Priall-O@ulster.ac.uk](mailto:De_Priall-O@ulster.ac.uk)

13 ***Abstract***

14 Small-scale gasification Combined Heat and Power systems, fed by biowaste resources, have  
15 the potential to enhance local renewable energy production, reduce carbon emissions and  
16 address the challenges of waste disposal. However, there is a lack of understanding on the  
17 influence of challenging feedstocks, such as, for example, digestate, poultry litter and  
18 municipal solid waste, on the syngas quality and the incidence of the drying stage in the overall  
19 process. This paper addresses this gap by analysing and comparing 40 samples of the most  
20 common biowaste feedstocks. We developed a stoichiometric-thermodynamic one stage  
21 equilibrium model that was experimentally validated and calibrated by laboratory results, with  
22 a maximum error of 15% between real and predicted values. Simulation results show that the

23 low heating value of the syngas produced from biowaste resources analysed ranges from 3.1 to  
24 5.4 MJ/Nm<sup>3</sup> on a dry basis. Working at the optimal equivalence ratio increases the electricity  
25 and thermal output by up to 20%. To achieve a feedstock moisture content of 10%, the drying  
26 process may require up to 60% of the heat produced. Furthermore, results show that downdraft  
27 gasification based combined heat and power, is a feasible and interesting option to deal with  
28 biowaste resources which can potentially avoid the cost, risk and externalities of landfilling  
29 while it contributes to the increase of local electricity and heat production from renewable  
30 energy sources, both for grid and off-grid applications.

### 31 ***Keywords***

32 Biowaste; Energy from waste; Gasification; Synthesis gas; Combined Heat and Power  
33 production

### 34 ***1. Introduction***

35 The use of biowaste for energy generation can play a significant role in decarbonisation of the  
36 energy system and waste reduction (Cheng et al., 2020). The potential of biowastes in  
37 industrialized countries is vast but remains unexploited, as highlighted by new guidance in the  
38 EU for energy production from waste (European Commission (EC), 2017). Although the  
39 implementation of source separated collection and new management strategies is expected to  
40 help reduce mixed waste streams, recent studies (Kaza et al., 2018) suggest that the generation  
41 of waste will continue to increase in the EU. Therefore, it is necessary to look at technological  
42 solutions that can transform local biowaste (e.g., food & food processing waste, agriculture  
43 residues, sewage sludge) into energy. Among the technologies for energy recovery from  
44 biowaste, it has been recognized that small-scale gasification units (around 200kWe) can play  
45 a key role in energy recovery processes by enabling a better use of local and regional biomass  
46 resources (Situmorang et al., 2020). Gasification is the thermochemical conversion of solid fuel

47 into gaseous products and is recognised as being among the highest technologies readiness  
48 level (TRL) systems for the conversion of biowaste into energy and fuels (Lovrak et al., 2020).  
49 Yao et al., (2018) found that compared to other thermochemical conversion methods,  
50 gasification technology has several advantages such as higher conversion efficiencies and  
51 minimal pollutants released to the atmosphere.

52 A significant increase in installed and operational downdraft gasifiers coupled with internal  
53 combustion engines (ICE's) around Europe recently is because of greater confidence in the  
54 technology, the availability of favourable subsidies and locally available biomass (Patuzzi et  
55 al., 2016). Installations can be found in Sweden, Germany, Finland and Italy (Patuzzi et al.,  
56 2021). Small-scale downdraft gasifiers have been identified as the most suitable set up for the  
57 feedstock types analysed in this study, as they have a simple design and can accept a wide  
58 variety of biomass materials (Elsner et al., 2017). Downdraft operation creates the least amount  
59 of tar, which can cause fouling in downstream equipment.

60 Many studies have discussed the potential of using biowastes, such as industrial wastes (Ayol  
61 et al., 2019; Galvagno et al., 2019), mixed solid waste (Arafat and Jijakli, 2013) and wood  
62 waste (Littlejohns et al., 2020) for syngas production. However, there is a scarcity of studies  
63 that have compared challenging biowaste resources (i.e., anaerobic digestate, poultry litter,  
64 municipal solid waste (MSW), agriculture and forestry residues) and investigated the main  
65 parameters influencing the quality of the syngas produced. While gasification of biowaste in  
66 small gasification ICE units has high potential to effectively generate heat and electricity, prior  
67 to the use of biowaste, especially wet waste, as a feedstock for gasification, a pre-treatment  
68 step is required to reduce its moisture content (MC) (Zhuang et al., 2020). Even fewer studies  
69 have discussed the incorporation of a drying stage in the whole gasification Combined Heat  
70 and Power (CHP) process, assuming it uses part of the heat produced by the CHP unit for pre-  
71 treatment purposes.

72 The paper aims to fill the gaps identified, by investigating optimal conditions for heat and  
73 electricity production from different types of biowastes using small-scale downdraft  
74 gasification coupled with ICE. Using a combination of experimental and mathematical  
75 modelling techniques, the paper analyses the performance of the entire system, when using  
76 challenging biowaste feedstocks and examines the opportunity to reuse the heat produced by  
77 the ICE system for pre-treatment purposes.

78 For the modelling efforts, we have chosen a thermodynamic model for the gasification process,  
79 as they are the simplest (from the viewpoint of their construction and solving) models  
80 developed and are most widely used in modelling studies (Ramos et al., 2019). They are easily  
81 customizable and converge rapidly, showing in most cases a good agreement with experimental  
82 data. The results produced by thermodynamic models are usually viewed as best case scenarios  
83 of gasification outcomes. We included small modifications (considering tar formation (Costa  
84 et al., 2015), assigning a fraction of the biomass carbon to char/methane formation (Li et al.,  
85 2001), adjusting the chemical reactions' equilibrium constants (Jarunthammachote and Dutta,  
86 2007)) to improve the accuracy of a thermodynamic equilibrium model and make it more  
87 suitable for the purpose of this work. None of the studies referenced above considered ash as a  
88 component participating in gasification and neither used their own experimental data to  
89 calibrate the modified models. The combination of modelling and experimental studies  
90 proposed in this paper is implemented and tested for the first time.

91 The novelty of the paper arises from the prediction of the effect of 40 biowaste samples, which  
92 differ in either waste types or characteristics (e.g., carbon, moisture, ash content), on the  
93 combined gasification-CHP process performance. A recent review (Ramos et al., 2019) found  
94 that only about 8% of modelling studies on gasification are concerned with wastes, while the  
95 majority of studies have been focused on biomass gasification (37%), followed by coal (24%).  
96 The modelling results have been experimentally validated using two types of biowastes (i.e.,

97 poultry litter and digestate) and published literature data. This enabled the development of a  
98 wider picture of the real potential of using biowaste in small-scale gasification CHP systems.  
99 We were also able to contextualise the incidence of the pre-treatment process on the overall  
100 energy conversion process.

## 101 **2. *Materials & Methods***

102 The work has been carried out through a combination of experimental analysis and  
103 mathematical modelling. This section discusses the models developed, the experimental  
104 apparatus, the rationale for feedstock selection and model validation efforts.

### 105 **2.1 Simulation of the biomass gasification-ICE system**

106 The modelled system consists of the following sub-systems: (a) biomass drying; (b) fixed-bed  
107 gasification reactor; (c) CHP module.

108 The CHP module is modelled using a black box. We assume that the ICE and heat recovery  
109 unit efficiencies are 30% ( $\eta_{el}$ ) and 52% (Patuzzi et al., 2016), respectively. For the CHP  
110 module, thermal energy discharged from the engine can be recovered using an engine  
111 coolant/water heat exchanger and an exhaust/water heat exchanger and used in the drying  
112 process (Caresana et al., 2011). We assume that the parasitic load represents 15% of the  
113 electricity production (Patuzzi et al., 2016)

114 The construction of the mathematical models for drying and gasification are detailed in the  
115 following sub-sections, a schematic of the fully coupled drying-gasification-CHP system is  
116 presented in the Supplementary Material, Figure S1.

#### 117 **2.1.1. *Biomass drying model***

118 Most common types of biomass and biowaste have a high MC, negatively impacting on their  
119 gasification behaviour and resulting syngas yield and quality (Tuomi et al., 2019). While

120 preliminary drying is necessary for proper gasification performance, it is a costly and energy  
121 intensive process (Cummer and Brown, 2002). The choice of drying equipment and  
122 optimization of drying conditions are essential for improving energy efficiency and  
123 profitability of a biomass cogeneration plant.

124 For the small-scale CHP gasification installation studied, we developed the modelling around  
125 the use of a belt dryer with hot air as the drying agent. Belt dryers are favoured for smaller  
126 drying applications, and can treat various materials, useful for co-gasification of biowastes  
127 (Fagernäs et al., 2010).

128 The dryer model is assembled writing the corresponding mass and energy balances, assuming  
129 the belt dryer uses hot air as the drying agent, adapting the system proposed by Holmberg and  
130 Ahtila (2005) to exclude a thermal recovery unit. The humid air exiting the drier is recirculated  
131 and heat losses are assumed to be 30% (Galvagno et al., 2016).

132 The schematics and full system of drying equations are presented in the Supplementary  
133 Material, Figure S1 and Table S1, respectively.

134 We assume the humid air exiting the dryer is fully saturated, and its humidity ( $Hum_{air}$ ) can be  
135 expressed function of the saturated vapour pressure ( $P_{sat}$ ), using Eq. 1.

$$136 \quad Hum_{air} = 0.622 \cdot P_{sat} / P_{air} \quad (1)$$

137 The saturated vapour pressure is expressed function of the air saturation pressure  $T_{air}$ , using  
138 Antoine's law, Eq. 2, where A, B and C are the values for the Antoine's coefficient.

$$139 \quad P_{sat} = 10^{A - \frac{B}{C + T_{air}}} \quad (2)$$

140 We assume that the temperature of biomass exiting the dryer is 10 °C lower than humid air.

141 The full system of equations, together with drying parameters and values/ranges used in the

142 calculations are supplied in the Supplementary Material, Table S1. The system of non-linear  
143 equations is solved using Matlab's built in function *fsolve*.

### 144 *2.1.2 Gasification model implementation and calibration*

145 Several reviews have been published, detailing thermodynamic models' construction (La  
146 Villetta et al., 2017; Safarian et al., 2019), applications (Baruah and Baruah, 2014; Puig-  
147 Arnavat et al., 2010), solving algorithms (Ramos et al., 2019). While we do not intend to  
148 reproduce them in this study, we highlight several references consulted to justify our choice of  
149 the mathematical model.

150 Thermodynamic models have been employed to compare biomass types and link biomass  
151 elemental composition to gasification performance: Vaezi et al. (2012) used a thermodynamic  
152 model to predict the heating values of syngas generated based on the ultimate analysis of 80  
153 biomass types. Despite successfully validating their model against other literature sources, they  
154 did not consider ash as a biomass constituent nor tar or char formation. Soltani et al., (2013)  
155 proposed and analysed a biomass integrated fired combined-cycle, comparing the performance  
156 of five materials: wood, paper, MSW, paddy husks and coal. Xu et al. (2017) investigated the  
157 gasification behaviour of seven types of MSW and three gasifying agents (air, hydrogen and  
158 steam). Both studies have successfully validated their models against published literature data.

159 Thermodynamic models have been employed to optimise operating conditions, saving time  
160 and expense associated with experimental efforts. Using a non-stoichiometric model,  
161 Gambarotta et al. (2018) investigated the influence of forestry waste characteristics and  
162 operating parameters on the syngas heating values. They found that lower gasification  
163 temperatures produce higher calorific value syngas (but did not report the temperature effect  
164 on gas yield) and higher concentrations of minor pollutants (ammonia, cyanide, COS).

165 Several assumptions inherent to thermodynamic models (i.e. reaching thermodynamic  
166 equilibrium, assuming no tar and char formation, isothermal gasification reaction) make them  
167 over-predict the formation of H<sub>2</sub> and CO and under-predict CH<sub>4</sub>.

168 Analysing the balance between the advantages (ease of implementation and solving,  
169 satisfactory accuracy, flexibility) and disadvantages (over-estimation of hydrogen production  
170 and under-estimation of methane formation), we have decided to use a stoichiometric  
171 thermodynamic equilibrium model in this study, and modify it, to enhance its prediction  
172 capability.

173 The equilibrium model developed follows a classic approach, proposed by Zainal et al. (2001),  
174 which assumes gasification to be a one-stage process and combines all the reactions into a  
175 general equation.

176 There are several underlying assumptions used for the general gasification equation. Firstly,  
177 biomass can be represented as three components: dry ash-free biomass with generic elemental  
178 formula  $CH_xO_yN_zS_u$ , ash and moisture (received from the drying unit). Ash does not take part  
179 in gasification and is included only in the heat balance equation. If the gasification temperature  
180 reaches ash melting temperature, it can lead to bed agglomeration and slagging phenomena, as  
181 noted by several experimental works (Gregorio et al., 2014; Katsaros et al., 2019). For  
182 biowastes with a high ash content this can lead to significant operating problems. Another issue  
183 related to ash is its heavy metal content, which can lead to corrosion problems. Heavy metals  
184 can accumulate in the ash and char residue, making their valorisation or disposal difficult (Chen  
185 et al., 2017). Chlorine content poses another problem for biowaste gasification, as HCl content  
186 in syngas varies according to experimental conditions and biomass type, from as low as 12  
187 ppm (Hervy et al., 2021) to over 1000 ppm (Turn, 2007).

188 We assume the sulphur biomass content is recovered as H<sub>2</sub>S, while nitrogen biomass content

189 is transformed solely to nitrogen gas. While several studies have reported ammonia and  
190 hydrogen cyanide formation from the nitrogen content in biomass, this varies according to  
191 biomass type: Vonk et al. (2019) reported syngas ammonia concentrations ranging from 619  
192 to 2107  $\mu\text{mol/mol}$ . Hervy et al. (2021) reported ammonia concentration of 115  $\text{mg/Nm}^3$  in  
193 syngas following solid recovered fuel gasification but higher concentrations of hydrogen  
194 cyanide (310 – 470  $\text{mg/Nm}^3$ ). These values are sufficiently small to justify neglecting  $\text{NH}_3$  and  
195 HCN contribution to gasification modelling.

196 Despite no limits being given for the syngas content of  $\text{H}_2\text{S}$ ,  $\text{NH}_3$  or  $\text{HCl}$  in ICE's, the pollutants  
197 have a negative effect on the environment and equipment. The consideration of pollutants' fate  
198 doesn't significantly affect model performance (and thus was neglected in the modelling effort)  
199 but must be kept in mind when considering gas cleaning.

200 We have included three of the model modification methods outlined above (tar formation,  
201 biomass carbon fraction to char and methane, and adjusting chemical reaction equilibrium  
202 constants), to bring model results closer to experimental ones. To the best of the authors'  
203 knowledge, Aydin et al., (2017) is the only study that proposed similar model modifications,  
204 while Costa et al. (2015) only considered tar formation and multiplicative factors for the  
205 equilibrium constants.

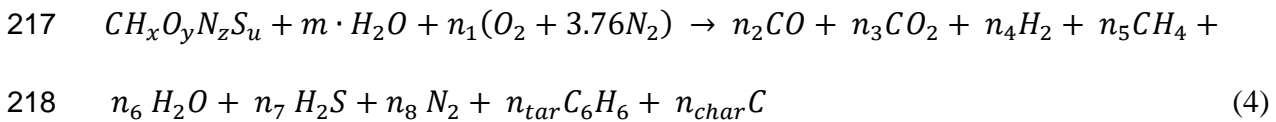
206 We amend the general equation to account for tar production (assuming tar can be represented  
207 by benzene), using the equation proposed by Costa et al. (2015) to calculate the corresponding  
208 tar coefficient (Eq.3).

$$209 \quad n_{tar} = 35.98 \exp(-0.0029 * T) \quad (3)$$

210 where T is the gasification temperature ( $^{\circ}\text{C}$ )

211 Then, we modify the model to assign part of the original biomass carbon content to the  
 212 formation of char (assumed to consist only of carbon) and methane, as proposed by Li et al.  
 213 (2001) and Aydin et al. (2017).

214 The modified general gasification reaction equation is written according to Eq. 4, further  
 215 enabling us to write the corresponding elemental mass balance for carbon, oxygen and  
 216 hydrogen.



219 Sulphur contribution is low in the biowastes considered (<1% wt) and can be neglected in the  
 220 energy balance equation. The amount of H<sub>2</sub>S formed during gasification is computed directly  
 221 from the elemental balance of the general gasification equation. We assume H<sub>2</sub>S can be  
 222 recovered entirely during gas cleaning and doesn't impact the CHP engine's functioning.  
 223 Poultry litter's high calcium content will assist with reduction of sulphur emissions, through  
 224 sequestration of sulphur in the ash (Dalólio et al., 2017). Similarly, the calcium/potassium  
 225 content in the ash can catalyse ammonia decomposition to N<sub>2</sub>.

226 We consider two chemical reactions representative of the gasification phenomena: the  
 227 homogeneous water – gas shift reaction (Eq.6) and the methanation reaction (Eq. 7).



230 The values for their equilibrium constants ( $K_1$  and  $K_2$ ) are expressed as a function of  
 231 temperature, according to Trninić et al. (2020), Eq. 8 and 9:

$$232 \quad \ln K_1 = 4276/T - 3.961 \quad (7)$$

233  $\ln K_2 = \frac{7082.848}{T} - 6.567 \cdot \ln T + 3.733e - 3 \cdot T - 0.3067e - 6 \cdot T^2 + 0.355e -$   
 234  $5/T^2 + 32.541$  (8)

235 Equilibrium equations for the two reactions are appended to the elemental mass balances, with  
 236 two further modelling assumptions: biomass and air are fed to the reactor at atmospheric  
 237 pressure and pressure drop in the reactor is negligible.

238 The final step in assembling the model is adding the heat balance equation (Eq. 9).

239  $\sum_{i=reactants} n_i h_{f,i}^0 = \sum_{i=products} n_i (h_{f,i}^0 + \Delta h_{T,i}^0)$  (9)

240 where  $h_{f,i}^0$  represents the formation enthalpy for reactants (including ash) and products and  
 241  $\Delta h_{T,i}^0$  is the enthalpy difference between the initial state (inlet to the gasification reactor) and  
 242 the gasification state (Eq. 10).

243  $\Delta h_{T,i}^0 = \Delta T \cdot C_{P,i}$  (10)

244 Where  $\Delta T$  represents the difference between inlet temperature to the gasifier and the  
 245 gasification temperature and  $C_{P,i}$  is the specific heat capacity of the participating species.

246 We also consider heat losses in the reactor and assume they represent 20% of inlet thermal  
 247 energy.

248 To solve the thermodynamic model, either the gasification temperature or the equivalence ratio  
 249 (ER) must be specified. Workings and merits of both these algorithms are comprehensively  
 250 detailed in Mendiburu et al. (2014).

251 For the simulations presented in this paper we specify the air ER and compute the resulting  
 252 gasification temperature, together with syngas composition. We chose to use the ER as an  
 253 input to the model, instead of temperature because, depending on reactor geometry and

254 operating conditions, temperature may not be constant in the reduction zone of the gasifier. In  
 255 contrast, for continuously operated gasifiers, the ER remains constant throughout the process.  
 256 Thus, we decouple the mass and energy balances and starting with a guess temperature we  
 257 solve the mass balance system of 5 equations to compute the coefficients for H<sub>2</sub>, CO, CO<sub>2</sub>,  
 258 CH<sub>4</sub> and H<sub>2</sub>O. Using the determined coefficients, we solve the energy balance equation to  
 259 compute temperature. If the difference between the initial and computed temperature is  
 260 smaller than 1K we assume the solving algorithm has converged successfully. If not, we  
 261 compute a new guess temperature (the mean value between the former guess temperature and  
 262 its calculated value) and perform another calculation step.  
 263 To examine the efficiency of the gasification system, we compute the syngas lower heating  
 264 value (LHV<sub>gas</sub>) and the cold gas efficiency (CGE), Eq. 11-12.

$$265 \quad LHV_{gas} = 10.8 x_{H_2} + 12.64 x_{CO} + 35.82 x_{CH_4}, \text{ MJ/Nm}^3 \quad (11)$$

266 where  $x$  represents the molar fraction of the component in the gas mixture

267 We do not consider tar contribution to the syngas' LHV, assuming tars can be completely  
 268 removed through syngas cleaning.

$$269 \quad CGE = \frac{LHV_{gas} \cdot G_{m,gas}}{LHV_{biomass} \cdot G_{m,biomass}} \cdot 100\% \quad (12)$$

## 270 **2.2 Experimental Apparatus**

271 The Fluidyne MicroLab Class Gasifier is an air blown gasifier operating at atmospheric  
 272 pressure, as presented in Figure 1.

273 The internal reactor diameter is 155 mm and height 165mm. The heart module houses the throat  
 274 plate, reduction tube and grate. Six air inlet manifolds introduce the gasification agent (air) to  
 275 the reactor, with flow rate controlled by an external handle. Syngas passes from the heart to the  
 276 blast tube where cooling occurs before the cyclone. The cyclones direct gas two ways: one

277 toward the test flare where a tap siphons it for cleaning and analysis, the other to an internal  
278 condenser and filtration system for engine application. Each module contains an outlet port for  
279 particulate removal. Pressure changes across the system are monitored using manometer  
280 connections. Thermocouples connected to the hearth, blast and cyclones record temperature  
281 evolution across the system, using a Grant 2020 series Squirrel data logger.

282 For analysis, gas is fed through the ETG PSS 100 Portable Sampling System Gas treatment  
283 equipped with Dreschel and Chiller scrubber system to remove remaining tar and particulates.  
284 Cleaned gas passes through the ETG MCA 100 Syn Biogas Multigas Analyzer, returning the  
285 CO<sub>2</sub>, CO, H<sub>2</sub>, N<sub>2</sub> and O<sub>2</sub> content as volumetric percentages.

### 286 **2.3 Feedstocks**

287 Poultry litter and AD digestate were selected for the analysis. All materials were pelletized to  
288 increase energy density and avoid bridging in the grate. Digestate was obtained from an AD  
289 plant run on a mixture of animal manure and green waste, the most common feedstock across  
290 Northern Ireland. Physical and chemical properties of the biowastes were analysed using  
291 relevant standard methods: MC (BS-EN ISO 18134), ash content (BS-EN ISO 18122) and  
292 volatile matter (VM) (BS-EN ISO 18123), through a Carbolite AAF 1100 Oven. Fixed carbon  
293 (FC) content was calculated by difference. Calorific Value (BS-EN ISO 18125) was  
294 determined using an IKA C200 calorimeter. Ash Melting (BS-EN ISO 21404) was carried out  
295 using a Carbolite CAF Digital Ash Melting Oven. Major elemental components Carbon (C),  
296 Hydrogen (H), Nitrogen (N) and Sulphur (S) were identified by means of a PE 2400 CHNS  
297 Elemental Analyser. Oxygen (O) content was calculated by difference. A laboratory in Belfast  
298 (ASEP, 2019) carried out the ultimate analysis for the two biowastes used for model validation.  
299 Results showed that poultry litter carbon content was 41.97%, while digestate pellets contained  
300 44.49% carbon. This difference could be due to the heterogenous mix of materials in each

301 biowaste such as feathers and bedding material in the poultry litter. Similar observations can  
302 be made regarding the hydrogen content of the materials. The determined higher heating values  
303 (HHV) (dry and ash free) are 18.15 MJ/kg for the poultry litter pellet and 22.32 MJ/kg for the  
304 digestate. The LHVs are 17.19 MJ/kg for the poultry litter pellet, 20.44 MJ/kg for miscanthus,  
305 and 20.97 MJ/kg for the digestate pellet. MC was 10.27% and 7.70% respectively, while ash  
306 content was 12.93% and 11.18% for each. Full results of the analysis are presented in  
307 supplementary material Table S4.

## 308 **2.4 Model Validation**

309 To perform model validation experiments, the gasification reactor was initially fed with  
310 approximately 0.6 kg of poultry litter/digestate pellets. We operated the reactor autothermally,  
311 initially heating the feedstock to 120 – 150 °C using a heat gun. After reaching this initial  
312 temperature, the heat gun is removed, and air is supplied to the gasifier. After an initial warm-  
313 up period (5 – 15 minutes, depending on biowaste type), the temperature reaches 850 – 950 °C.  
314 To ensure longer and consistent operation, we refilled the reactor, whenever the temperature  
315 probes recorded steep increases/decreases in temperature. On average, the gasifier was refilled  
316 every 15-20 minutes with ~ 200 g fresh biowaste. After each experiment, the contents of the  
317 reactor and gas cooling and cleaning system were inspected. The reactor was cleaned, and the  
318 amount of char, ash and tar was weighted.

319 The experimental results show on average a relatively consistent quality syngas with LHVs  
320 between 3.14 – 3.8 MJ/Nm<sup>3</sup> in the case of digestate and 2.84 – 4.15 MJ/Nm<sup>3</sup> in the case of  
321 poultry litter. This low heating value is due to the experimental conditions, where the air  
322 flowrate was relatively high, diluting the syngas and lowering its overall calorific value.  
323 Because of the small scale of the experimental set-up, the air flow rate to the gasifier was  
324 difficult to control and optimize during experimental operation.

325 For model calibration/validation, we recorded the operation intervals in which the syngas  
326 composition and temperature read-outs remained relatively constant and the initial model  
327 outcomes were compared to the average experimental values.

328

329 Figure 2 shows the comparison between the percentage of CH<sub>4</sub>, CO, CO<sub>2</sub>, H<sub>2</sub> obtained using  
330 the experimental set up and the model. The results are reported on a dry basis, nitrogen making  
331 up the rest to 100% of the syngas. The experimental outcomes reported in Figure 2 are the  
332 average of three experimental runs in similar conditions.

333 The model calibration was performed using an ER of 0.48, which was found to best represent  
334 the experimental results. As this is a batch process it is difficult to determine the ER using the  
335 experimental setup accurately: when biomass is consumed during gasification, the ER  
336 increases (the air flow rate remaining constant). When the reactor is refilled, the ER decreases.  
337 The high value comes from the fact that the gasifier deployed is not equipped with a system to  
338 control the air intake and has high thermal losses. The ER of 0.48 was obtained comparing the  
339 experimental results (gas composition, gasification temperature) with those obtained through  
340 modelling, choosing the ER value which minimised the departure between modelling and  
341 experimental results. Despite this being high for a gasification process, the corresponding  
342 temperature calculated using the thermodynamic model was a 1175°C in the case of the  
343 digestate and 1285 °C for the chicken litter pellets. The temperature ranges in which the  
344 experimental results were recorded were 820 – 1030 °C for digestate and 920 – 980 °C for the  
345 chicken litter experiments. The temperature sensor was placed above the gasification zone, so  
346 the temperature recorded was lower than the one registered in the gasifier. Additionally, the  
347 ±10% experimental error makes us confident to use of the proposed ER in the model validation  
348 efforts. Due to the difficulty in controlling the air supply to the reactor, we were unable to

349 optimize the experimental runs further to obtain a higher gas quality. We used the validated  
350 mathematical model to simulate what would happen in a larger scale reactor with proper air  
351 supply control and similar design characteristics to our laboratory set-up.

352 The operation temperature being higher than the ash melting temperature determined  
353 experimentally, but we did not observe any ash agglomeration in the reactor.

354 To bring the model results closer to experimental ones, we used the method proposed by  
355 Jarungthammachote and Dutta (2007), multiplying the values of the equilibrium constants for  
356 the two chemical reactions rates ( $K_1$  and  $K_2$  presented in Eq. 8 and 9, respectively) considered  
357 in the model with two model coefficients ( $p_1$  and  $p_2$ ). To determine the values of the two  
358 coefficients, we employed genetic algorithm optimisation (Houck et al., 1995). We chose to  
359 use genetic algorithms, as they are less likely to converge to local minima and can search a  
360 larger parameter space; they are more flexible because they do not depend on the structure of  
361 the optimization problem and they do not require a continuous parameter space. Genetic  
362 algorithm optimization has been shown to outperform classical methods in several fields  
363 (Martínez et al., 1996). For the minimization function we used the root mean square deviation  
364 between model and experimental data. We used Matlab's own genetic algorithm optimization  
365 function *ga* ("Genetic Algorithm Homepage," R2021a.). The values of the two regression  
366 coefficients were  $p_1 = 4.69$  and  $p_2 = 4.26$ .

367 Following model calibration, there is a very good model-experiment agreement in the case of  
368 the digestate: the standard relative error between modelling and experimental values is between  
369 2 and 28% and the root mean squared deviation is 1.99. The largest model experiment departure  
370 is observed in the case of hydrogen. The poultry litter data also shows good performance (with  
371 standard errors between 6.5 and 15.5%) with a root mean squared deviation of 2.42. To verify  
372 the model predictions against independent literature sources, we selected several of the

373 references presented in Trninić et al.(2020) and Aydin et al. (2017), and compared our own  
374 model predictions against them. Results, showing a good agreement between model and  
375 experiments, similar to other modelling studies, are listed in Table S2.

### 376 **3. Results and Discussion**

377 Aiming to understand the potential of heat and electricity production from local biowaste  
378 through small gasification units combined with ICE, we identified the most common biowaste  
379 types and divided them into five categories: poultry litter, digestate, MSW, agricultural wastes  
380 and forestry residues. The potential of these biowastes in the UK is presented in the  
381 supplementary material, Table S3, to provide an idea of local resources available for energy  
382 production from waste.

383 We have analysed multiple literature sources and identified 40 different biowaste resources for  
384 the different categories considered. For each biowaste category, we have considered multiple  
385 samples as their ultimate and proximate composition can vary widely, depending on origin,  
386 time of year, weather and cultivation conditions. It is worth noting that poultry litter, digestate  
387 and MSW show the highest variability of parameters considered, and for this reason we  
388 selected a higher number of samples. We selected 12 samples for MSW, 9 for digestate and  
389 poultry litter, 8 for agricultural residues and 2 for forestry residues. The full table with the  
390 different biowaste resources, their ash, moisture and elemental compositions, together with the  
391 references consulted, is provided in the Supplementary Material, Table S4.

392 To investigate and quantify the influence of varying biowaste composition on the biowaste  
393 gasification suitability, we simulated their gasification behaviour in similar conditions: using  
394 an ER of 0.35 and assuming all biomass types have been dried prior to gasification to a MC of  
395 10%. We analysed the effect of each biowaste ash content, nitrogen content, C:H and C:O  
396 ratio on the syngas yield and calorific value. The full results from the simulations (gas

397 compositions, heating value and dry yield) for each biowaste samples are presented in the  
398 Supplementary Material, Table S5.

### 399 3.2.1. Ash content

400 While ash does not actually take part in the gasification reactions (as long as the gasification  
401 temperature does not reach ash melting temperature), it has a significant impact of gasification  
402 performance. Firstly, biowastes with low ash content, have a higher amount of ‘true’ biomass  
403 available for gasification and thus will produce higher gas yields. This is shown in Figure 3a,  
404 where the dry syngas yield shows a relatively linear decrease with increasing biowaste ash  
405 content.

406 Biowaste ash acts as a heat sink during the gasification process and lowers the gasification  
407 temperature. Lower gasification temperature results in a decreased formation of hydrogen and  
408 carbon monoxide, which in turn lowers the heating value of the syngas. Methane concentration  
409 increases at lower temperatures, but the increase is not sufficient to overcome the lower  
410 concentrations of both hydrogen and carbon monoxide. As a result, the calorific value of the  
411 syngas will decrease at high biowaste ash content.

412 As seen in Figure 3b, biowastes with high ash content generally produce syngas with lower  
413 heating value. For example, the digestate sample, characterised by an ash content of 65%,  
414 shows one of the lowest values of LHV ( $3.5 \text{ MJ/Nm}^3$ ).

415

416 Exceptions are given by samples that are characterised by either high or low level of carbon  
417 content that can offset the effect of the ash content. An example is one of the samples of  
418 MSW (i.e. organic waste, carbon content 53% w) that shows one of the highest LHV ( $5.4$   
419  $\text{MJ/Nm}^3$ ), although the ash content is 40% (w). Other examples are the samples of poultry

420 litter and MSW with a low carbon content, around 29% (w) and, although the ash content is  
421 below 20%, the LHV is below 4 MJ/Nm<sup>3</sup>.

422

### 423 3.2.2. Ultimate composition analysis

424 The elemental composition of biomass plays an important role in the evaluation of syngas  
425 composition and calorific value. The gasification knowledge predicts that biowastes with low  
426 C:H ratio, high C:O ratios and as well as a low N content will produce the highest LHV syngas.  
427 However, the model results show that the amount of any single element does not have a clear  
428 influence on the LHV of the syngas produced, but rather the combination of them all. It is  
429 therefore important to run several experiments before assessing the real gasification potential  
430 of a specific biowaste.

431 While biowastes with a high oxygen content (low C:O ratio) typically have lower heating  
432 values, the simulation results indicate that the same does not hold true for the heating values of  
433 the syngas produced via gasification (Figure 4a). Neither the C:O nor C:H ratio (Figure 4b)  
434 appear to have a distinguishable effect on the distribution of syngas LHVs. The influence of  
435 nitrogen is also puzzling: while for most biowaste types high N-content lowers the syngas  
436 LHV, the poultry litter samples with high nitrogen content (6-8%) do not appear to follow this  
437 downward trend (Figure 4c). Simulation results confirm that the higher the hydrogen content  
438 of the biowaste (lower C:H ratio), the higher the H<sub>2</sub> concentration in the syngas (Figure 4d).

### 439 3.2.3. Moisture content and drying performance

440 Operational experience requires a maximum MC of 20% for a downdraft gasifier. However,  
441 based on empirical experience, the recommended value to allow the smooth operation of the  
442 gasifier is 10%. We have tested the influence of MC on gasification performance for biowastes  
443 with final MC in the range 5 – 20%, assuming an ER of 0.25 The results were similar for all

444 biowaste types, but for clarity we focused on the poultry litter sample which produced the  
445 highest LHV syngas and cold gas efficiency, selected from Katsaros et al. (2019).

446 For higher MC, the syngas composition is characterised by higher H<sub>2</sub> concentrations, as well  
447 as higher CO<sub>2</sub>. Despite this, the decrease in CO concentration leads to a small overall decrease  
448 in the syngas heating value, accompanied by incrementally higher gas yield and lower cold gas  
449 efficiency (Table 1).

450 Overall, as shown in Table 1, a higher biomass MC entering the gasification reactor has little  
451 impact on the amounts of heat and electricity generated through the ICE. The heat requirement  
452 for drying the biomass from its initial MC increases significantly as the target moisture  
453 becomes lower, reaching the 25% of the heat recovered by the CHP unit when a 5% MC is  
454 required. Unless better heat integration is considered (e.g. using the flue gases as the drying  
455 medium, employing solar drying) the need to reduce the MC to such a level could lower the  
456 plant's profit margins.

457

#### 458 3.2.4. Equivalence Ratio

459 To investigate the influence of the ER, we selected the best performing poultry litter sample,  
460 with a MC of 10% and varied the ER between 0.15 and 0.5. High ERs lead to high gasification  
461 temperatures, which promote the formation of CO from the water gas shift reaction (to the  
462 detriment of H<sub>2</sub> formation) and lower the rate of the methanation reaction. As a result, the  
463 syngas LHV will decrease with increasing ERs (Figure 5a). On the other hand, low ERs (and  
464 thus lower temperatures) favour pyrolysis reactions and result in low gas yields (Figure 5a).

465 Figure 5a. shows that there is an optimum equivalence ratio to maximise the gasification  
466 efficiency, as well as overall CHP performance, shown in Figure 5b. Working at the optimal

467 ER (Figure 5b) can provide an increase in the electricity and heat produced, with a difference  
468 between the minimum and maximum energy output achievable by more than 20%.

### 469 3.2.5. Overall Performance Comparison

470 To compare the different feedstocks and understand their potential for electricity and heat  
471 production, we assumed a 100 kg/h of as received biomass, optimized the ER for all categories.  
472 Full results for each biowaste sample (syngas yield, LHV and CHP output) are presented in the  
473 Supplementary Material, Table S5.

474 Table 2 shows the main output of the gasification process combined with an ICE for the best  
475 performing biowaste samples in the categories considered. The difference between biowastes  
476 that require drying prior to gasification (digestate, poultry litter, food and garden waste) and  
477 those that do not (forestry and agricultural residues) is highlighted. For forestry and agriculture  
478 residues, the natural drying process in an open area would be enough to bring the MC below  
479 20% (Ramachandran et al., 2017).

480 The MC of the digestate, poultry litter sample and MSW is of 40%, 30% and 50%, respectively.  
481 Meaning that for 100 kg/h of as received feedstock, the dried biomass represents only 40, 70,  
482 and 50 kg/h, respectively. Consequently, the syngas energy content available for samples of  
483 the digestate, poultry litter and MSW is lower than the ones for agriculture and forestry  
484 residues. The digestate requires the highest percentage of the heat produced, that is almost 60%.

485

486 Results show that using biowaste in gasification cogeneration systems is feasible, providing  
487 electricity and heat that can contribute to low carbon energy production. The economy of the  
488 investment depends on the specific case study, but increasing cost of waste disposal, as shown  
489 by the UK value of the gate fee (Letsrecycle, 2021) will further help the business case.  
490 Furthermore, the solution investigated in this study provides an alternative pathway to

491 landfilling. There are applications where investing in gasification cogeneration systems is  
492 already economically viable. We provide an example using a poultry litter gasification CHP  
493 system for electricity and heat production.

494 To understand the economic feasibility, we assumed a case study with four standard broiler  
495 sheds (73m x 18m) containing 27,000 birds per shed (Caslin, 2016) and developed a simplified  
496 techno-economic analysis. Each shed host 8 crops of birds annually. Technical and economic  
497 parameters used are summarised in Table 3.

498 We considered the poultry litter previously analysed and assumed to run the gasifier at the  
499 optimal ER. Through on-site conversion of biowaste to energy, a farm switching to a small-  
500 scale downdraft plant combined with an ICE could introduce a 350kW gasifier coupled to a  
501 120kW ICE. The CO<sub>2</sub> savings would be of about 490 tonnes of CO<sub>2</sub> per year. Savings are from  
502 avoiding the purchase of LPG and grid electric for energy needs. Further savings come from  
503 exporting electric back to the grid. The farm would be, therefore, able to cover the cost for the  
504 thermal and electrical demand of the poultry houses shown in Table 5, with some revenue  
505 coming from the electricity produced that is not used on site. For the exporting tariff, we  
506 assumed a value of £0.03/kWh, that could be agreed with the energy provider. It is worth noting  
507 that selling a high amount of electricity to the grid would be challenging and not feasible in  
508 congested areas. In our simplified case study, the return of investment would be below 11 years,  
509 due to the high cost of LPG that is commonly used to cover the energy needs of poultry houses,  
510 and export prices per tonne of poultry litter for disposal (Assembly, 2012).

#### 511 **4. Conclusions**

512 The study analysed the production of electricity and heat from biowaste resources in a small  
513 gasification unit with the aim of showing the potential for reusing local renewable sources to  
514 address the problem of waste disposal. The authors acknowledge that thermodynamic models

515 are limited in their predictions, as they cannot consider reactor set-up, mass, heat and  
516 momentum transfer limitations or the entire set of chemical reactions that occur. However, we  
517 believe the findings of this paper can be used as a benchmark for the performances of small-  
518 scale gasification units combined with ICE.

519 Results show that the drying is essential for biowastes with high MC (50 – 60%), such as  
520 poultry litter, digestate and MSW. The incidence of the drying stage on the whole process could  
521 be high. The heat required to reduce the MC to 10% for the samples analysed ranges from 19%  
522 to 60% of the thermal energy produced by the CHP, with the maximum value required by  
523 digestate.

524 In cases of high thermal demand, the use of alternative low-energy drying systems, such as  
525 solar energy and microwave pre-heating systems is critical to allow for all the heat generated  
526 to be used for the local heating load.

527 The LHV of the syngas produced by the 40 feedstocks ranges from 3.1 to 5.4 MJ/Nm<sup>3</sup>.  
528 Although this value is low, the syngas produced must be considered as a value-added product  
529 of a waste resource. Some biowastes, such as digestate and poultry litter, will also avoid  
530 the environmental impact and the externalities of disposing of hazardous biomaterials directly  
531 to the environment.

532 Results highlight the importance of running a preliminary test for assessing the real  
533 syngas potential of any biowaste resource. The single amount of oxygen, carbon, hydrogen,  
534 or nitrogen, do not allow for an accurate prediction of the gasification potential.

535 Rather than the single element composition, it is the mix of different elements which determine  
536 the LHV of the syngas produced.

537 Running the gasifier at the optimal ER is important, with a 20% difference in  
538 the energy outcomes from the CHP unit between best and worst-case scenarios.

539 Agriculture and forestry residues do not require any pre-treatment drying process and can

540 produce a useful quantity of electricity. The finding highlights the potential applications of  
541 such biowastes for off-grid electricity and heat production as discussed in Verkerk et al., (2019)

## 542 **Acknowledgements**

543 The authors acknowledge the support of the Bryden Centre project. The Bryden Centre project  
544 is supported by the European Union's INTERREG VA Programme, managed by the Special  
545 EU Programmes Body (SEUPB).

## 546 **Disclaimer**

547 The views and opinions expressed in this paper do not necessarily reflect those of the European  
548 Commission or the Special EU Programmes Body (SEUPB).

## 549 **Bibliography**

550 Arafat, H.A., Jijakli, K., 2013. Modeling and comparative assessment of municipal solid waste  
551 gasification for energy production. *Waste Manag.* 33, 1704–1713.  
552 <https://doi.org/10.1016/j.wasman.2013.04.008>

553 ASEP, 2019. ASEP Facilities [WWW Document]. State Art Facil. Instrum.

554 Assembly, N.I., 2012. Poultry Litter Utilisation and Disposal: Alternative Technologies to Fluidised  
555 Bed Combustion [WWW Document].

556 Aydin, E.S., Yucel, O., Sadikoglu, H., 2017. Development of a semi-empirical equilibrium model for  
557 downdraft gasification systems. *Energy* 130. <https://doi.org/10.1016/j.energy.2017.04.132>

558 Ayol, A., Tezer Yurdakos, O., Gurgen, A., 2019. Investigation of municipal sludge gasification  
559 potential: Gasification characteristics of dried sludge in a pilot-scale downdraft fixed bed  
560 gasifier. *Int. J. Hydrogen Energy* 44, 17397–17410.  
561 <https://doi.org/10.1016/j.ijhydene.2019.01.014>

562 Baruah, D., Baruah, D.C., 2014. Modeling of biomass gasification: A review. *Renew. Sustain. Energy*  
563 *Rev.* <https://doi.org/10.1016/j.rser.2014.07.129>

564 Caresana, F., Brandoni, C., Feliciotti, P., Bartolini, C.M., 2011. Energy and economic analysis of an  
565 ICE-based variable speed-operated micro-cogenerator. *Appl. Energy* 88, 659–671.  
566 <https://doi.org/10.1016/j.apenergy.2010.08.016>

567 Caslin, B., 2016. Energy Efficiency on Poultry Farms.

568 Chen, G., Guo, X., Cheng, Z., Yan, B., Dan, Z., Ma, W., 2017. Air gasification of biogas-derived  
569 digestate in a downdraft fixed bed gasifier. *Waste Manag.* 69, 162–169.  
570 <https://doi.org/10.1016/j.wasman.2017.08.001>

571 Cheng, S.Y., Tan, X., Show, P.L., Rambabu, K., Banat, F., Veeramuthu, A., Lau, B.F., Ng, E.P., Ling,  
572 T.C., 2020. Incorporating biowaste into circular bioeconomy: A critical review of current trend  
573 and scaling up feasibility. *Environ. Technol. Innov.* 19, 101034.  
574 <https://doi.org/10.1016/j.eti.2020.101034>

575 Costa, M., Villetta, L., Massarotti, N., 2015. Optimal Tuning of a Thermo-Chemical Equilibrium  
576 Model for Downdraft Biomass Gasifiers, in: *CHEMICAL ENGINEERING TRANSACTIONS*.  
577 <https://doi.org/10.3303/CET1543074>

578 Cummer, K.R., Brown, R.C., 2002. Ancillary equipment for biomass gasification. *Biomass and*  
579 *Bioenergy*. [https://doi.org/10.1016/S0961-9534\(02\)00038-7](https://doi.org/10.1016/S0961-9534(02)00038-7)

580 Dalólio, F.S., Nogueira, J., Cássia, A., Oliveira, C. De, De, I., Ferreira, F., Christiam, R., Oliveira, M.  
581 De, Teixeira, F., Teixeira, S., 2017. Poultry litter as biomass energy : A review and future  
582 perspectives. *Renew. Sustain. Energy Rev.* 76, 941–949.  
583 <https://doi.org/10.1016/j.rser.2017.03.104>

584 DEFRA, 2020. UK Government GHG Conversion Factors for Company Reporting. London.

585 Elsner, W., Wysocki, M., Niegodajew, P., Borecki, R., 2017. Experimental and economic study of  
586 small-scale CHP installation equipped with downdraft gasifier and internal combustion engine.  
587 *Appl. Energy* 202, 213–227. <https://doi.org/10.1016/j.apenergy.2017.05.148>

588 European Commission (EC), 2017. Communication from the Commission to the European

589 Parliament, the Council, the European Economic and Social Committee and the Committee of  
590 the Regions - The role of waste-to-energy in the circular economy. COM(2017) 34 final.  
591 26.1.2017. COM/2017/0034 Final 1–11. <https://doi.org/10.1002/bdd.453>

592 Fagnäs, L., Brammer, J., Wilén, C., Lauer, M., Verhoeff, F., 2010. Drying of biomass for second  
593 generation synfuel production. *Biomass and Bioenergy*.  
594 <https://doi.org/10.1016/j.biombioe.2010.04.005>

595 Galvagno, A., Prestipino, M., Maisano, S., Urbani, F., Chiodo, V., 2019. Integration into a citrus juice  
596 factory of air-steam gasification and CHP system: Energy sustainability assessment. *Energy*  
597 *Convers. Manag.* 193, 74–85. <https://doi.org/10.1016/j.enconman.2019.04.067>

598 Galvagno, A., Prestipino, M., Zafarana, G., Chiodo, V., 2016. Analysis of an Integrated Agro-waste  
599 Gasification and 120 kW SOFC CHP System: Modeling and Experimental Investigation. *Energy*  
600 *Procedia* 101, 528–535. <https://doi.org/10.1016/J.EGYPRO.2016.11.067>

601 Gambarotta, A., Morini, M., Zubani, A., 2018. A non-stoichiometric equilibrium model for the  
602 simulation of the biomass gasification process. *Appl. Energy* 227, 119–127.  
603 <https://doi.org/10.1016/j.apenergy.2017.07.135>

604 Genetic Algorithm Homepage [WWW Document], n.d. URL  
605 <https://uk.mathworks.com/help/gads/genetic-algorithm.html> (accessed 5.28.21).

606 Gregorio, F. Di, Santoro, D., Arena, U., 2014. The effect of ash composition on gasification of poultry  
607 wastes in a fluidized bed reactor: <https://doi.org/10.1177/0734242X14525821> 32, 323–330.  
608 <https://doi.org/10.1177/0734242X14525821>

609 Hervy, M., Remy, D., Dufour, A., Mauviel, G., 2021. Gasification of Low-Grade SRF in Air-Blown  
610 Fluidized Bed: Permanent and Inorganic Gases Characterization. *Waste Biomass Valorization*  
611 2021 1, 1–14. <https://doi.org/10.1007/S12649-021-01434-W>

612 Holmberg, H., Ahtila, P., 2005. Evaluation of energy efficiency in biofuel drying by means of energy  
613 and exergy analyses. *Appl. Therm. Eng.* 25, 3115–3128.

614 <https://doi.org/10.1016/j.applthermaleng.2005.04.005>

615 Houck, C.R., Joines, J.A., Kay, M.G., 1995. A Genetic Algorithm for Function Optimization: A  
616 Matlab Implementation.

617 Jarungthammachote, S., Dutta, A., 2007. Thermodynamic equilibrium model and second law analysis  
618 of a downdraft waste gasifier. *Energy* 32, 1660–1669.  
619 <https://doi.org/10.1016/J.ENERGY.2007.01.010>

620 Jeswani, H.K., Whiting, A., Martin, A., Azapagic, A., 2019. Environmental and economic  
621 sustainability of poultry litter gasification for electricity and heat generation. *Waste Manag.* 95,  
622 182–191. <https://doi.org/10.1016/j.wasman.2019.05.053>

623 Katsaros, G., Pandey, D.S., Horvat, A., Almansa, G.A., Fryda, L.E., Leahy, J.J., Tassou, S.A., 2019.  
624 Gasification of poultry litter in a lab-scale bubbling fluidised bed reactor: Impact of process  
625 parameters on gasifier performance and special focus on tar evolution. *Waste Manag.* 100, 336–  
626 345. <https://doi.org/10.1016/j.wasman.2019.09.014>

627 Kaza, S., Yao, L., Bhada-Tata, P., Van Woerden, F., 2018. What a Waste 2.0: A Global Snapshot of  
628 Solid Waste Management to 2050, 經濟研究. The World Bank. [https://doi.org/10.1596/978-1-](https://doi.org/10.1596/978-1-4648-1329-0)  
629 4648-1329-0

630 La Villetta, M., Costa, M., Massarotti, N., 2017. Modelling approaches to biomass gasification: A  
631 review with emphasis on the stoichiometric method. *Renew. Sustain. Energy Rev.*  
632 <https://doi.org/10.1016/j.rser.2017.02.027>

633 Letsrecycle, 2021. EfW, landfill, RDF 2021 gate fees [WWW Document]. [letsrecycle.com](https://letsrecycle.com).

634 Li, X., Grace, J.R., Watkinson, A.P., Lim, C.J., Ergüdenler, A., 2001. Equilibrium modeling of  
635 gasification: A free energy minimization approach and its application to a circulating fluidized  
636 bed coal gasifier. *Fuel*. [https://doi.org/10.1016/S0016-2361\(00\)00074-0](https://doi.org/10.1016/S0016-2361(00)00074-0)

637 Littlejohns, J. V., Butler, J., Luque, L., Austin, K., 2020. Experimental Investigation of Bioenergy  
638 Production from Small-Scale Gasification of Landfill-Diverted Wood Wastes. *Waste and*

639 Biomass Valorization. <https://doi.org/10.1007/s12649-020-00940-7>

640 Lovrak, A., Pukšec, T., Duić, N., 2020. A Geographical Information System (GIS) based approach for  
641 assessing the spatial distribution and seasonal variation of biogas production potential from  
642 agricultural residues and municipal biowaste. *Appl. Energy* 267, 115010.  
643 <https://doi.org/10.1016/j.apenergy.2020.115010>

644 Martínez, M., Senent, J., Blasco, X., 1996. A Comparative Study of Classical Vs Genetic Algorithm  
645 Optimization Applied in GPC Controller. *IFAC Proc. Vol. 29*, 1769–1774.  
646 [https://doi.org/10.1016/S1474-6670\(17\)57925-2](https://doi.org/10.1016/S1474-6670(17)57925-2)

647 Mendiburu, A.Z., Carvalho, J.A., Coronado, C.J.R., 2014. Thermochemical equilibrium modeling of  
648 biomass downdraft gasifier: Stoichiometric models. *Energy*.  
649 <https://doi.org/10.1016/j.energy.2013.11.022>

650 Patuzzi, F., Prando, D., Vakalis, S., Rizzo, A.M., Chiamonti, D., Tirlor, W., Mimmo, T., Gasparella,  
651 A., Baratieri, M., 2016. Small-scale biomass gasification CHP systems: Comparative  
652 performance assessment and monitoring experiences in South Tyrol (Italy). *Energy* 112, 285–  
653 293. <https://doi.org/10.1016/j.energy.2016.06.077>

654 Puig-Arnabat, M., Bruno, J.C., Coronas, A., 2010. Review and analysis of biomass gasification  
655 models. *Renew. Sustain. Energy Rev.* 14, 2841–2851.  
656 <https://doi.org/10.1016/J.RSER.2010.07.030>

657 Ramachandran, S., Yao, Z., You, S., Massier, T., Stimming, U., Wang, C.H., 2017. Life cycle  
658 assessment of a sewage sludge and woody biomass co-gasification system. *Energy* 137, 369–  
659 376. <https://doi.org/10.1016/j.energy.2017.04.139>

660 Ramos, A., Monteiro, E., Rouboa, A., 2019. Numerical approaches and comprehensive models for  
661 gasification process: A review. *Renew. Sustain. Energy Rev.*  
662 <https://doi.org/10.1016/j.rser.2019.04.048>

663 Safarian, S., Unnpórsson, R., Richter, C., 2019. A review of biomass gasification modelling. *Renew.*

664 Sustain. Energy Rev. <https://doi.org/10.1016/j.rser.2019.05.003>

665 Situmorang, Y.A., Zhao, Z., Yoshida, A., Abudula, A., Guan, G., 2020. Small-scale biomass  
666 gasification systems for power generation (<200 kW class): A review. *Renew. Sustain. Energy*  
667 *Rev.* <https://doi.org/10.1016/j.rser.2019.109486>

668 Soltani, S., Mahmoudi, S.M.S., Yari, M., Rosen, M.A., 2013. Thermodynamic analyses of a biomass  
669 integrated fired combined cycle. *Appl. Therm. Eng.* 59, 60–68.  
670 <https://doi.org/10.1016/j.applthermaleng.2013.05.018>

671 Trninić, M., Stojiljković, D., Manić, N., Skreiberg, Ø., Wang, L., Jovović, A., 2020. A mathematical  
672 model of biomass downdraft gasification with an integrated pyrolysis model. *Fuel* 265, 116867.  
673 <https://doi.org/10.1016/j.fuel.2019.116867>

674 Tuomi, S., Kurkela, E., Hannula, I., Berg, C.G., 2019. The impact of biomass drying on the efficiency  
675 of a gasification plant co-producing Fischer-Tropsch fuels and heat – A conceptual  
676 investigation. *Biomass and Bioenergy* 127, 105272.  
677 <https://doi.org/10.1016/j.biombioe.2019.105272>

678 Turn\*, S.Q., 2007. Chemical Equilibrium Prediction of Potassium, Sodium, and Chlorine  
679 Concentrations in the Product Gas from Biomass Gasification. *Ind. Eng. Chem. Res.* 46, 8928–  
680 8937. <https://doi.org/10.1021/IE071040F>

681 Vaezi, M., Passandideh-Fard, M., Moghiman, M., Charmchi, M., 2012. On a methodology for  
682 selecting biomass materials for gasification purposes. *Fuel Process. Technol.* 98, 74–81.  
683 <https://doi.org/10.1016/j.fuproc.2012.01.026>

684 Verkerk, P.J., Fitzgerald, J.B., Datta, P., Dees, M., Hengeveld, G.M., Lindner, M., Zudin, S., 2019.  
685 Spatial distribution of the potential forest biomass availability in europe. *For. Ecosyst.* 6.  
686 <https://doi.org/10.1186/s40663-019-0163-5>

687 Vonk, G., Piriou, B., Wolbert, D., Cammarano, C., Vaïtilingom, G., 2019. Analysis of pollutants in  
688 the product gas of a pilot scale downdraft gasifier fed with wood, or mixtures of wood and waste

689 materials. *Biomass and Bioenergy* 125, 139–150.  
 690 <https://doi.org/10.1016/J.BIOMBIOE.2019.04.018>

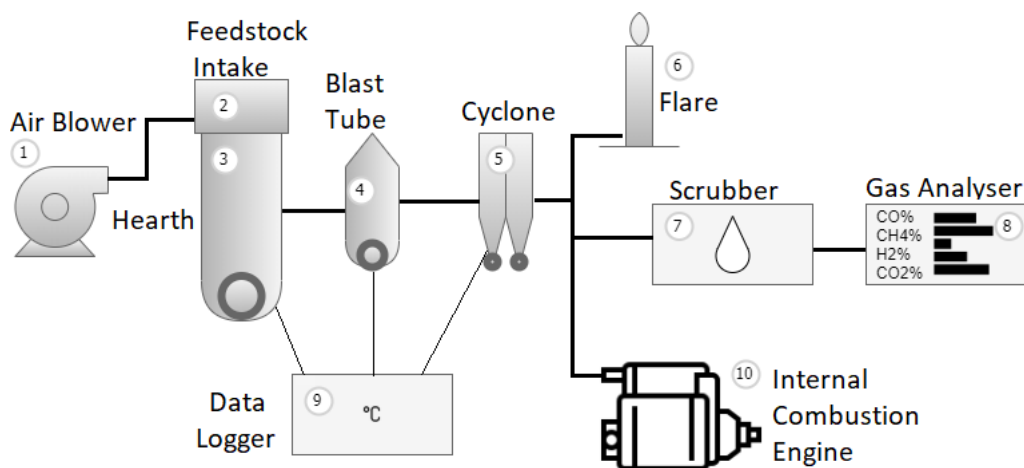
691 Xu, P., Jin, Y., Cheng, Y., 2017. Thermodynamic Analysis of the Gasification of Municipal Solid  
 692 Waste. *Engineering* 3, 416–422. <https://doi.org/10.1016/J.ENG.2017.03.004>

693 Yao, Z., You, S., Ge, T., Wang, C.-H., 2018. Biomass gasification for syngas and biochar co-  
 694 production: Energy application and economic evaluation. *Appl. Energy* 209, 43–55.  
 695 <https://doi.org/10.1016/j.apenergy.2017.10.077>

696 Zainal, Z.A., Ali, R., Lean, C.H., Seetharamu, K.N., 2001. Prediction of performance of a downdraft  
 697 gasifier using equilibrium modeling for different biomass materials. *Energy Convers. Manag.*  
 698 42, 1499–1515. [https://doi.org/10.1016/S0196-8904\(00\)00078-9](https://doi.org/10.1016/S0196-8904(00)00078-9)

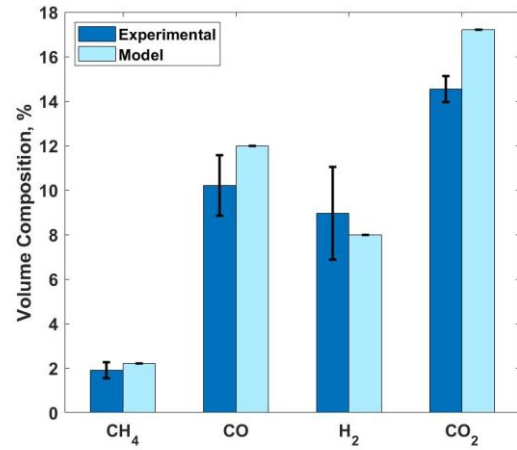
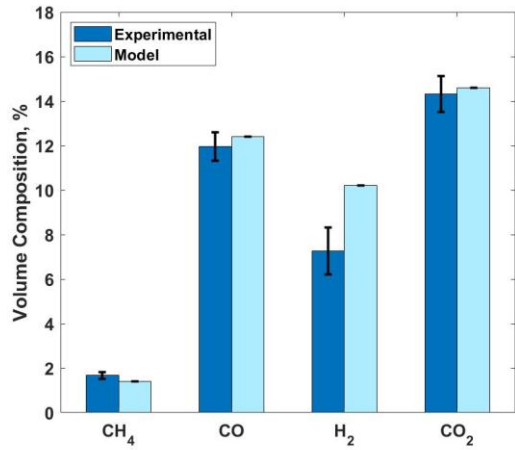
699 Zhuang, X., Song, Y., Zhan, H., Yin, X., Wu, C., 2020. Gasification performance of biowaste-derived  
 700 hydrochar: The properties of products and the conversion processes. *Fuel* 260, 116320.  
 701 <https://doi.org/10.1016/j.fuel.2019.116320>

702



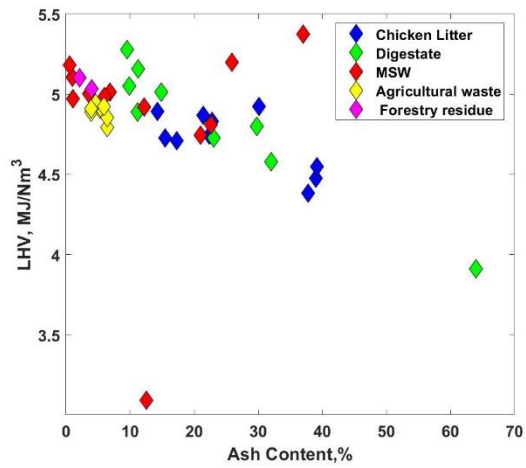
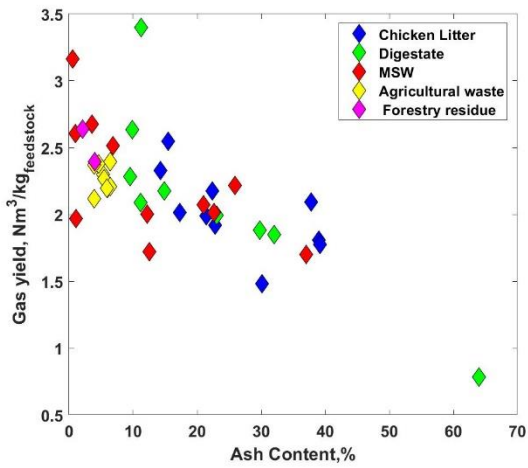
703

704 *Figure 1. Experimental Apparatus Set Up*



705

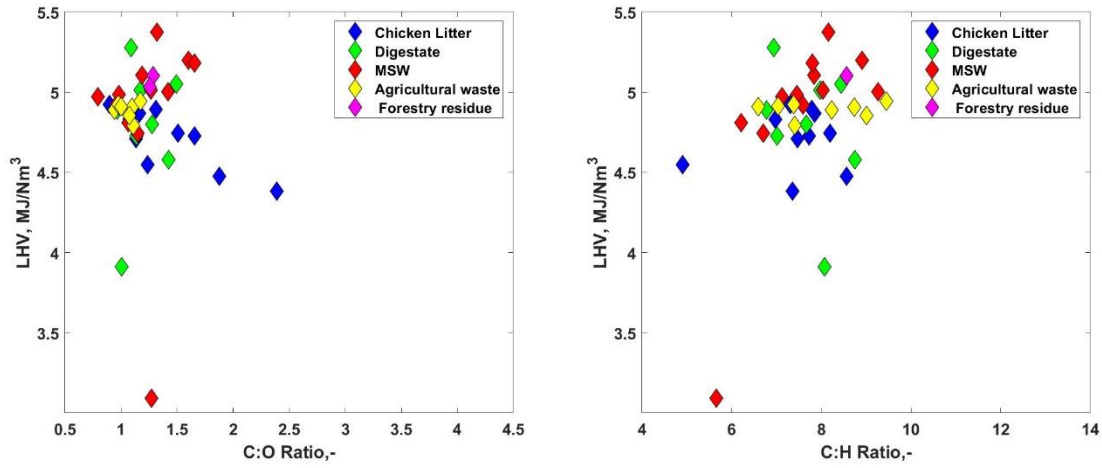
706 *Figure 2. Model Validation for a. Digestate and b. Poultry Litter experiments*



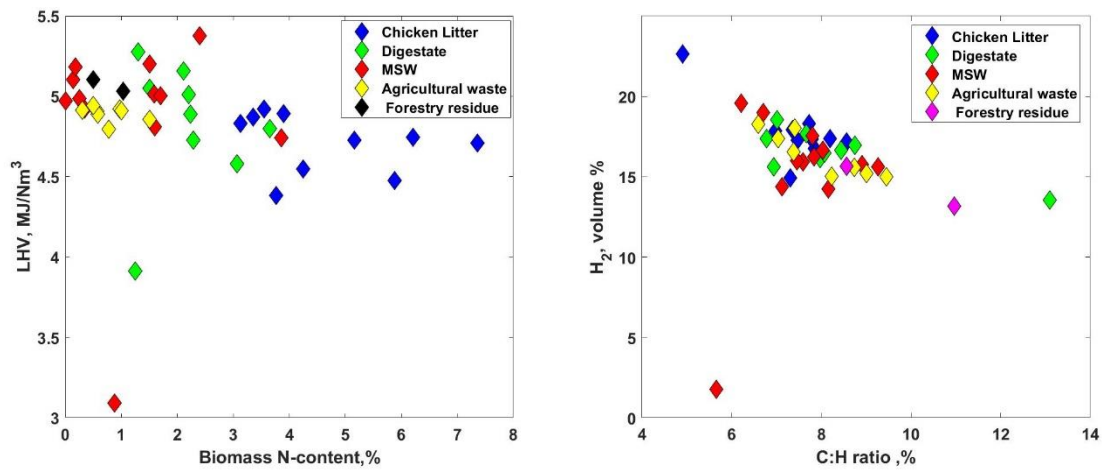
707

708 *Figure 3. Influence of biomass ash content on a. dry syngas yield and b. syngas LHV*

709



710



711 *Figure 4. Influence of a. C:O ratio, b. C:H ratio c. N-Content on syngas LHV and d.*

712 *influence of C:H ratio on the syngas H<sub>2</sub> content*

713 **Table 1. Influence of moisture content on gasification-CHP performance for poultry**

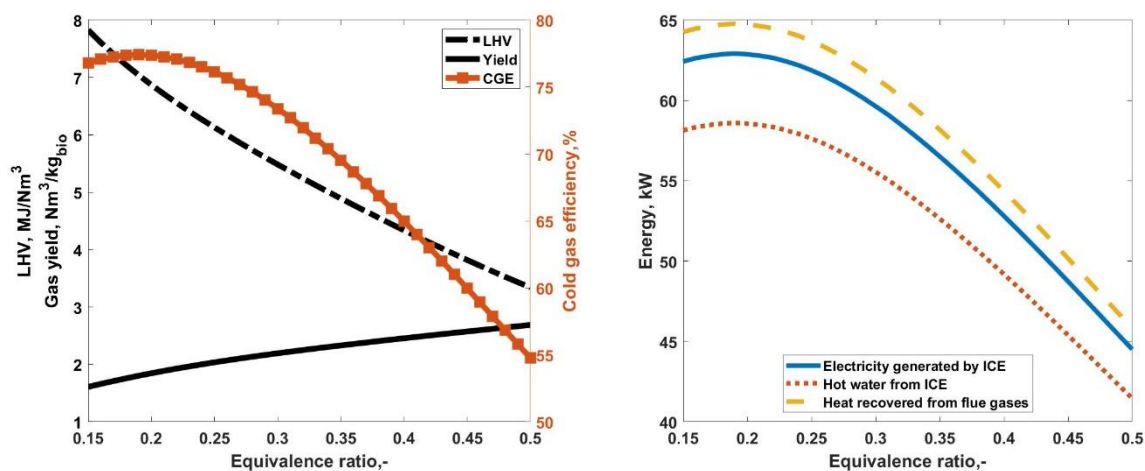
714 **litter defined in Katsaros et al. (2019).**

	Moisture content = 5%	Moisture content = 10%	Moisture content = 15%	Moisture content = 20%
H <sub>2</sub> (% vol)	19.7	20.6	21.4	22.2
CO (% vol)	20.6	19.4	18.3	17.3
CO <sub>2</sub> (% vol)	9.8	10.7	11.5	12.3
CH <sub>4</sub> (% vol)	2.3	2.3	2.2	2.2
LHV (MJ/Nm <sup>3</sup> )	5.55	5.49	5.42	5.36
Gas yield (Nm <sup>3</sup> /kg dry biomass)	2.17	2.19	2.22	2.24
Cold gas efficiency (%)	73.40	73.38	73.38	73.36

Heat for drying (kW)	29.25	23.74	18.22	12.67
Electricity (kW)	59.65	59.64	59.64	59.62
Hot water from ICE (kW)	61.41	61.39	61.39	61.37
Heat from flue gases (kW)	55.56	55.54	55.54	55.53

715 \*Boundary condition: 15°C and 1.013 bar

716



717 *Figure 5. Influence of equivalence ratio on a. syngas heating value, yield and cold gas*  
718 *efficiency. and b. CHP energy output for the sample defined in Katsaros et al. (2019)*

719

720 **Table 2. Comparison between different biowastes assuming a flow rate of 100 kg/h of as**  
721 **received biomass (best performing biowaste samples)**

Biowaste type	Moisture content (%)	Feedstock LHV** (MJ/kg)	Syngas energy content (kW)	Drying requirement (kW) (% on the total heat)	Net electricity (kW)	Heat as hot water (kW)	Heat from flue gases (kW)
Drying process required (10% MC target)							
Poultry litter	30%	16.4	246.3	23.7 (19%)	62.8	58.52	64.86
Digestate	60%	25.1	200.1	57.6 (58%)	51.01	47.51	52.51

Municipal Solid Waste	50%	23.2	260.5	46.3 (30%)	79.7	74.24	82.05
Drying process not required							
Agriculture residue (Wheat straw)	/	16.9	346.2	-	88.28	82.2	90.9
Forestry residues	/	19.4	390.4	-	99.56	92.7	102.5

722 \*\*Dry basis

723 \*\*\* T 15°C and 1.013 bar

724

725 **Table 3. Techno-economic parameters used for assessing the poultry litter case study**

<b>Technical parameters</b>	
<b>Parameter</b>	<b>Value</b>
<b>Boundary condition</b>	<b>15 °C, 1.013 bar</b>
<b>Baseline scenario (Caslin, 2016)</b>	
Birds per shed	27,000
Electricity demand per shed [MWh/year]	35
Thermal demand per shed [MWh/year]	240
Number of sheds	4
Poultry litter annually gathered per shed [tonne per year]	227
Electricity tariff [pence/kWh]	15.52
LPG cost [£/kWh]	0.07
CO <sub>2</sub> emission factor for the electricity bought from the grid kgCO <sub>2</sub> /kWh (DEFRA, 2020)	0.283
CO <sub>2</sub> emission factor LPG [kgCO <sub>2</sub> /kWh] (DEFRA, 2020)	0.23
<b>Poultry litter gasification CHP application</b>	
Gasifier efficiency at the optimal equivalence ratio	73%
Poultry litter LHV [kWh/kg]	4.16
Gasifier capacity for 4 Sheds [kW]	350
CHP capacity for 4 Sheds [kWe]	120
Annual Operational Hours	7,056
Electricity produced by the CHP for the entire site [MWh]	966
Thermal energy produced by the CHP for the entire site [MWh]	1,450
Electricity exported to the grid [MWh]	826
Gasification CHP Initial Investment [£] (Jeswani et al., 2019)	1,059,824
Maintenance Cost [£]	39,413
Contingency Cost [£]	105,982
Integration Cost [£]	317,947
Material Storage Cost [£]	20,000
Material Handling Cost [£/tonne]	4.00

Exported electricity tariff [£/kWh]	0.03
Tariff for litter disposal in Northern Ireland [£/tonne]	30
Simple Pay Back [years]	<11

726